

# PUGWO-TEABC-MNet: A Hybrid Metaheuristic Framework for Optimal Ice-Melting Device Placement in Power Distribution Networks

Yue Li<sup>1\*</sup>, Hao Yang<sup>2</sup>, Yaorong Hu<sup>3</sup>, Anjiang Liu<sup>1</sup>, Chen Dou<sup>1</sup>

<sup>1</sup>Electric Power Research Institute of Guizhou Power Grid Co., Ltd., Guiyang 550002, Guizhou, China

<sup>2</sup>China Southern Power Grid Co., Ltd., Guangzhou 510080, Guangdong, China

<sup>3</sup>Powerchina Guizhou Electric Power Engineering Co., LTD., Guiyang 550002, Guizhou, China

<sup>4</sup>guizhou Power Grid Co., LTD., Guiyang 550002, Guizhou, China

E-mail: 1641356033@qq.com, 1907977145@qq.com, 1907977145@qq.com, 1196570632@qq.com, klgjdou@126.com

\*Corresponding author

**Keywords:** PUGWO-TEABC-MNet, Ice-melting device placement, hybrid metaheuristics, power distribution networks, PCA, climatic prediction, reliability optimization

**Received:** September 8, 2025

*Ice accumulation on power distribution lines leads to significant reliability issues, operational instability, and economic losses during extreme weather conditions. Accurate prediction and optimal placement of ice-melting devices are essential to mitigate these impacts and ensure continuous power delivery. Conventional optimization approaches often exhibit slower convergence, limited adaptability to nonlinear climatic variations, and inadequate prediction accuracy under uncertain environmental parameters. The objective to develop an intelligent and robust hybrid framework for optimal ice-melting equipment placement, enhancing prediction precision and system resilience. A new hybrid metaheuristic framework, PUGWO-TEABC-MNet, is formulated by integrating a Position-Updated Grey Wolf Optimizer (PUGWO), Tent-Elite Artificial Bee Colony (TEABC), and LSTM-based Memory Network (MNet) to ensure adaptive exploration and exploitation with dynamic memory learning. The framework optimally determines device placement by minimizing prediction error while modeling nonlinear climatic dependencies. Climatic datasets related to icing events, including wind speed, temperature, humidity, and ice thickness, were collected from Kaggle repositories. Data were normalized and partitioned into an 80:20 training–testing ratio. Principal Component Analysis (PCA) was used to retain the eight most significant components representing climatic influence. PUGWO initializes optimal search regions, TEABC refines global optima, and MNet captures sequential temporal patterns to improve predictive stability. The framework was implemented in Python using TensorFlow and Scikit-learn libraries. Performance metrics achieved include  $R^2 = 0.992$ , MAPE = 0.0042, and RMSE = 0.12, outperforming baseline BP and PSO-BP approaches. The proposed framework demonstrates superior forecasting accuracy and resilience, providing a cost-effective strategy for optimal ice-melting device deployment in power distribution networks.*

*Povzetek: Predlagan hibridni model PUGWO-TEABC-MNet omogoča zelo natančno napovedovanje poledenitve in optimalno postavitev naprav za taljenje ledu, s čimer izboljšuje zanesljivost elektrodistribucijskih omrežij.*

## 1 Introduction

Transmission line icing can result in flashover, line disconnection, or tower collapse when supercooled water droplets hit conductors and freeze. Important variables like the collision coefficient and freezing fraction have a big impact on network dependability and ice buildup [1]. Ice buildup on transmission lines causes structural damage, conductor galloping, and outages, which complicate

maintenance plans during extended cold temperatures and high winds and result in financial losses, safety risks, and decreased power supply dependability [2]. Ice mitigation techniques include conductor or insulator protection strategies, hydrophobic surface treatments, monitoring systems, anti/de-icing technologies, and ice-melting devices. These strategies were developed to lessen electrical failures, mechanical disruptions, and extensive grid damage during severe icing events [3]. Ice-melting

devices improve distribution network reliability by addressing mechanical and thermal limitations, including AC and DC techniques; however, challenges such as power outages, complex switching, reactive power issues, and electromagnetic interference limit widespread use under severe icing conditions [4]. The placement of ice-melting devices is made more difficult by icing incidents, complicated terrain, high altitude conditions, and fluctuating weather patterns, since variables like temperature, wind speed, precipitation, and conductor diameter have a significant impact on ice formation and mitigation efficiency [5]. The best placement strategy is essential for reducing the risks of conductor galloping, flashover, and ice-shedding since precise placement of ice-melting devices improves suppression mechanisms, lowers mechanical stress, and increases the dependability of high-voltage transmission networks during extreme icing conditions [6]. In ice-melting systems, performance factors such as resilience metrics, composite cost, risk cost, and reliability indicators combine technical stability and economic efficiency to assess efficacy and direct the best choice of anti-icing techniques for transmission lines [7]. By balancing investment, operational efficiency, and mitigation effectiveness under extreme ice disaster scenarios, economic evaluation considerations include composite cost, risk cost, and coordination of de-icing with power grid scheduling, assuring robust distribution systems [8]. The combination of scientific and financial aspects requires integrating flexible grounding devices with controlled reactive current regulation, minimizing reliance on large-capacity power supplies while ensuring cost efficiency, operational reliability, and practical application in distribution systems under hazardous icing circumstances [9].

### 1.1 Research objective

An advanced Position-Updated Grey Wolf Optimizer with Tent-Elite Artificial Bee Colony-based Memory Network (PUGWO-TEABC-MNet) method was established in this research for optimal ice-melting device placement by integrating real-world distribution feeder data collection, Min–Max scaling, PCA-based feature reduction, and PUGWO-TEABC-MNet-driven climatic risk prediction, ensuring precise placement, enhanced convergence, network resilience, operational efficiency, and economically sustainable distribution system performance under extreme icing conditions.

### Research questionnaire

**RQ1:** Does the proposed hybrid metaheuristic algorithm outperform classical optimization techniques when used to

identify the optimal location of ice-melting devices in a scenario of climatic uncertainty?

**RQ2:** How does the incorporation of Tent mapping improve the convergence efficiency and solution accuracy of the Position-Updated Grey Wolf Optimizer?

**RQ3:** In what ways does the proposed model compare in terms of reliability, energy efficiency, and robustness with the current ice-melting placement strategies?

The remaining sections are structured as follows: Section 1 discusses the background and limitation of current ice-melting device installation strategies, Section 2 explores the literature review on icing risk prediction, Section 3 discusses data gathering, preprocessing, and feature extraction and the PUGWO-TEABC-MNet method proposed, then after that Section 4 involves experimental setup, results, and findings, and finally, Section 5 concludes with insights and directions for further research.

## 2 Related works

Icing thickness prediction of transmission lines was done with spectral clustering, Complete Ensemble Empirical Mode Decomposition with Adaptive Noise (CEEMDAN), and a Transformer model [10]. There was limited evaluation on various climatic regions, but results indicated better accuracy and efficient learning compared to baseline algorithms with multiple feature inputs. An integrated model driven by Artificial Intelligence (AI) was intended to forecast icing thickness in Sichuan based on multi-source meteorological and icing information [11]. Data assimilation enhanced prediction accuracy, but errors of more than 3 mm still existed, while the overall outcomes manifested high accuracy at the main observation stations. Acoustic wave de-icing to provide sustainable alternatives to traditional methods by piezoelectric plate experiments in laboratory and wind tunnel settings [12]. Limited scalability was a challenge, but findings presented synergistic effects of resonance frequency analysis and surface modification for real-time monitoring of icing. An extensive model used temperature, humidity, and past icing data to anticipate hard rime and glaze ice [13]. Despite erratic monitoring difficulties, the results showed that several icing kinds may be accurately predicted with greater accuracy than with traditional monitoring techniques. A flexible grounding device regulates zero-sequence reactive current in research [14] to allow de-icing without cutting power. Experiments report voltage deviation under 0.5% and current deviation under 0.3%, keeping the network running and showing economic benefits, though large-scale real-world validation was still limited. An FFNN-based model with optimization was

used in research [15] to estimate ice-to-liquid ratios and to plan anti-icing and de-icing operations. Simulations on IEEE 33-node networks show reduced load loss, sensitivity to weather factors, and overall better network performance, but operational testing and full scalability haven't been fully evaluated. The assessment of power grid icing risk was done using a probabilistic inference approach [16]. Although it was difficult to capture nonlinear development patterns, Poisson process modeling using Monte Carlo simulations showed that the proportions of ultra-high voltage lines and the thickness of the ice had a significant impact on the vulnerability of the system. A two-stage stochastic model is used in research [17] to maximize the dispatch of distributed energy resources and routing for mobile deicing equipment during ice storms. Scenario-based simulations on IEEE 33- and

69-node systems show improved resilience, although scalability to very large networks remains limited. An enhanced You Only Look Once version 8 (YOLOv8) network with bidirectional feature pyramid network (BiFPN) fusion and Gather-Excite (GE) attention was utilized to detect all-dielectric self-supporting (ADSS) cable icing [18]. Despite an increase in computational complexity, trials demonstrated improved early-warning capabilities, accuracy, and recall when compared to the previous model. AC de-icing of 10kV distribution network lines was examined with fixed, segmented, and mobile systems incorporating intelligent switches [19]. Applicability to higher conductor cross-sections was limited, but performance showed flexible deployment and efficient ice removal for differing line distances. Table 1 shows an overview of related works.

Table 1: Summary of the related works

Ref.	Method / Model	Application Focus	Dataset / Inputs	Performance / Metrics	Technical Limitations
Ke et al. [10]	CEEMDAN + Spectral Clustering + Enhanced Transformer	Transmission line icing thickness prediction	Meteorological & icing time-series	RMSE, R <sup>2</sup> (better than CEEMDAN-LSTM/SP-Transformer)	Limited climatic validation; may overfit specific regions
Wang et al. [11]	AI-based Integrated Model + Data Assimilation	Icing prediction in Sichuan power grid	Multi-source meteorological & icing data (2017 -2019)	Prediction error < 3 mm; R <sup>2</sup> ≈ 0.9	Regional overfitting; residual errors at some stations
Del Moral et al. [12]	Acoustic-Wave (AW) De-icing	Anti-icing/de-icing on piezoelectric substrates	Lab & wind-tunnel experiments	Energy efficiency > 90%; real-time response	Scalability was limited due to the lab hardware setup
Zhou et al. [13]	Multi-factor Prediction Model (Temp, Humidity, History)	Hard rime & glaze ice prediction	Historical icing cycles (9 locations)	Corr. > 0.99; MSE < 4%	Depends on sensor coverage & data quality
Luo & Zhou [14]	GBDT Regression Model	De-icing agent melting-area prediction	Indoor experiment data	R <sup>2</sup> = 0.979	Limited real-world applicability; no field testing
Snaiki et al. [15]	FFNN + Metaheuristic Optimizers	Ice-to-liquid ratio estimation	ASOS meteorological data	High accuracy; Sobol index sensitivity	Complex model; multiple optimizer tuning; not tested operationally
Liu et al. [16]	Poisson Process + Monte Carlo Simulation	Power-grid icing risk assessment	Simulated UHV grid data	Risk 15× for UHV lines (50%)	Nonlinear modeling; high computation; detailed grid data needed
Vangulick et al. [17]	Optimal Measurement Device Placement (ANM based)	Distribution network operation	Simulated network data	Reduced curtailment; improved ANM quality	Depends on ANM assumptions; may not generalize to other topologies
Kong et al. [18]	Improved YOLOv8 + GE & BiFPN	ADSS fiber icing detection	RGB images of optical fiber cables	Accuracy 2.2%, Recall 5%, FPS = 147	High computation; real-time deployment may be hardware-limited
Zhao et al. [19]	Two-Stage Stochastic Scheduling Model	Distribution network resilience under ice storms	Modified IEEE 33-/69-node system	Scenario-based improved resilience	Limited scalability for very large systems

## 2.1 Research gap

Despite significant progress, limitations remain across existing icing prediction and de-icing approaches. CEEMDAN showed that limited evaluation across diverse climatic regions existed [10]. AI-based models provided better predictions with data assimilation, although inaccuracies remained [11]. Acoustic wave de-icing had sustainable potential without scalability [12]. Multi-factor models forecast varied icing types, but irregular monitoring decreased dependability [13]. ML frameworks accurately quantified de-icing agents, albeit field applicability was limited [14]. Probabilistic risk models were poor at handling nonlinear growth patterns [16], yet cable detection using YOLOv8 enhanced accuracy but increased computational complexity [18]. Integrated, adaptive, and cost-effective solutions are still missing. To address the issues of traditional approaches, a PUGWO-TEABC-MNet method was developed to combine temporal pattern, leader updated exploration, tent-chaotic initialization, and elite-guided exploitation with the aim of improving the accuracy, resilience, and cost-effectiveness of deploying ice-melting devices in distribution systems for varying climate conditions.

## 3 Methodology

A hybrid method, PUGWO-TEABC-MNet, addresses optimal placement of ice-melting devices in distribution networks. Climatic and feeder data undergo Min–Max scaling and PCA-driven feature extraction. LSTM-supported MNet predicts icing risks, while PUGWO enhances exploration, and TEABC improves global convergence. The integrated model ensures accurate prediction, resilience, and cost-efficient placement. Figure 1 presents the overall framework.

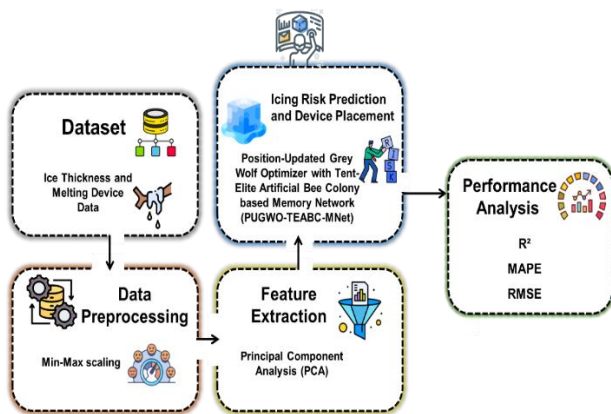


Figure 1: Methodology flow

## 3.1 Dataset

The ice thickness and melting device data were obtained from the open-source platform Kaggle (<https://www.kaggle.com/datasets/zara2099/ice-thickness-and-melting-device-data/data>). The dataset includes measurements of ice accumulation and removal on transmission lines. It covers environmental variables including temperature, humidity, and wind speed, as well as ice thickness measurements. Data also records the performance of ice-melting operations under various power grid configurations. The dataset is appropriate for investigating ice disaster warnings, power system reliability, and the operational efficiency of ice-melting equipment. The dataset was cleaned before analysis to eliminate missing values or unrealistic values. Min-max scaling and PCA were used to normalize features and eliminate the least important information to use in modeling.

## 3.2 Data preprocessing using min-max scaling

Min-Max scaling is employed as a crucial preprocessing technique to standardize continuous parameters linked with distribution networks, such as temperature, load demand, and cost. Min-Max scaling is a linear transformation technique that converts original feature values to a specified range, often ranging from 0 to 1, maintaining uniform relevance across variables. The transformation is expressed as Equation (1).

$$F_{scaled} = \frac{F_j - F_{low}}{F_{high} - F_{low}} \quad (1)$$

Where  $F_j$  and  $F_{scaled}$  represent the original and scaled feature value,  $F_{low}$  is the minimum, and  $F_{high}$  is the maximum of the feature range. Min–Max scaling allowed for dependable extraction and optimal placement of ice-melting devices in distribution networks by standardizing diverse data into equivalent units, improving stability, speeding up convergence, and guaranteeing balanced representation of meteorological, demand, and financial factors.

## 3.1. Principal component analysis (PCA) for feature extraction

PCA is a method of dimensionality reduction used for reducing high-dimensional climatic, load, and network variables to identify predominant patterns that affect ice accumulation within distribution networks. PCA converts correlated features  $V = V_1, V_2, \dots, V_n$  into uncorrelated

principal components (PCs), which constitute a rotated coordinate system to extract maximum variance. The first principal component  $P_1$ , is linearly composed of original variables derived in Equation (2).

$$P_1 = c'_1 V = c_{11}V_1 + c_{12}V_2 + \dots + c_{1n}V_n \tag{2}$$

Subsequent PCs are defined similarly in Equation

$$P_2 = c'_2 V = c_{21}V_1 + c_{22}V_2 + \dots + c_{2n}V_n, \dots, P_n = c'_n V \tag{3}$$

Where  $c_{ij}$  are coefficients derived from the eigenvectors of the covariance matrix  $\Sigma$  of  $V$ , and eigenvalues  $\lambda_1 > \lambda_2 > \dots > \lambda_n$  indicate the variance captured by each component. Variance and covariance are computed as in Equation (4).

$$\text{Var}(P_j) = c'_j \Sigma c_j, \text{Cov}(P_j, P_k) = c'_j \Sigma c_k \tag{4}$$

Table 2: Cumulative variance table

Principal Component	Eigenvalue	Variance (%)	Cumulative Variance (%)
$P_1$	3.42	62	62
$P_2$	1.41	25	87
$P_3$	0.55	10	97
$P_4$	0.20	3	100

The eigenvalue and cumulative variance analyses kept the two primary variables ( $P_1$  and  $P_2$ ), which account for 87% of the overall variation.  $P_1$  is a climatic factor, and  $P_2$  is a load factor, maintaining the important patterns that influence ice accumulation and reducing dimensionality. The retained components are those that have the greatest amount of variance, as indicated in Table 2, and it can be argued that these features should be used to reduce the number of features. PCA achieves feature dimensionality reduction with preservation of the most important information, allowing efficient and reliable feature extraction to predict icing threats. PCA improves convergence, decreases computational complexity, and enhances precision in optimizing the placement of ice-melting devices in distribution systems by highlighting prevailing climatic and operational trends.

### 3.4 Predict icing risks using Position-Updated Grey Wolf Optimizer with Tent-Elite Artificial Bee Colony based Memory Network (PUGWO-TEABC-MNet)

The proposed PUGWO-TEABC-MNet model forecasts the risks of icing and identifies the most appropriate location of ice-melting equipment within the power distribution networks. The MNet is a time-varying forecast of icing hazards at various network sites and is the first to predict these hazards. The PUGWO and TEABC algorithms, in their turn, are guided by these predictions. In particular, high-risk regions determined by MNet are prioritized more in the optimization process, and PUGWO and TEABC can efficiently explore device placements maximizing the melting and minimizing the cost. The interdependence of components will ensure that the temporal icing patterns are immediately factored into the optimization loops, culminating in a more precise and fiscally viable placement strategy shown in Figure 2.

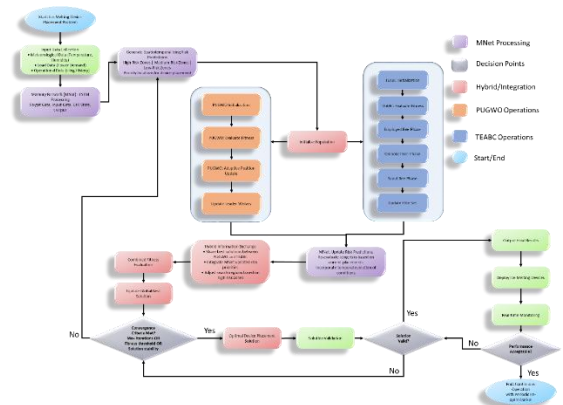


Figure 2: PUGWO-TEABC-MNet architecture for optimal device placement

#### 3.4.1 Memory networks (MNet)

MNets analyze temporal connections in meteorological, load, and operational data to predict icing risks and optimize the placement of ice-melting devices in distribution networks. Because it makes use of an LSTM method, vanishing gradient problems are avoided, and long-term dependencies are maintained. A hidden state and a cell state are present in every LSTM unit, which spreads information over time. The forget gate ( $F_t$ ) determines which prior knowledge should be discarded using Equation (5).

$$F_t = \sigma(A_f[H_{t-1}, Z_t] + B_f) \tag{5}$$

The input gate ( $I_t$ ) and candidate memory ( $N_t$ ) determine the new information to store, which can be derived in Equations (6-8).

$$I_t = \sigma(A_i[H_{t-1}, Z_t] + B_i) \quad (6)$$

$$N_t = \tanh(A_n[H_{t-1}, Z_t] + B_n) \quad (7)$$

$$C_t = C_{t-1} \cdot F_t + N_t \cdot I_t \quad (8)$$

For predictions, the hidden state ( $H_t$ ) is created by filtering the cell state using the output gate ( $O_t$ ) using Equations (9-10).

$$O_t = \sigma(A_o[H_{t-1}, Z_t] + B_o) \quad (9)$$

$$H_t = O_t \cdot \tanh(C_t) \quad (10)$$

Here,  $C_{t-1}$  and  $C_t$  are previous and current cell states,  $H_t$  and  $O_t$  are hidden and output states,  $A$  and  $B$  represent gate-specific weights and biases, and  $Z_t$  denotes the input vector of climatic, load, and operational features. MNet generates precise predictions of icing risk by capturing temporal patterns in temperature, load demand, and icing incidents. These forecasts help the PUGWO-TEABC method position ice-melting devices in the best possible way, improving distribution networks' cost-effectiveness, operational effectiveness, and network resilience.

### 3.4.2 Position-Updated Grey Wolf Optimizer (PUGWO)

GWO is a meta-heuristic optimization algorithm derived from the grey wolf's social ordering and hunting behavior. Wolves are divided into Alpha, Beta, Delta, and Omega, corresponding to the fittest, second-fittest, third-fittest, and least-fit solutions. The algorithm imitates three phases of hunting: encircling the prey, pursuing the prey, and approaching the prey, leading the population towards the best solution in the search space; it mainly helps to forecast the transmission line's risk of ice. The standard GWO is prone to premature convergence and local optimum stagnation caused by the uniform impact of leader wolves and reduced exploration in early iterations. To overcome this, the PUGWO adjusts the position update mechanism through the introduction of adaptive weight coefficients depending on the fitness values of Alpha ( $\alpha$ ), Beta ( $\beta$ ), and Delta ( $\delta$ ) wolves, reflecting hierarchical influence on

device placement in a distributed network. A random term can have an impact on early-stage exploration by other wolves to balance global and local search. The new position update formula is derived in Equations (11-14).

$$Y_k^{t+1} = \alpha_1 \cdot r_1 \cdot \frac{(v_\alpha Z_\alpha + v_\beta Z_\beta + v_\delta Z_\delta)}{3} + \alpha_2 \cdot (Y_k^t + r_2 \cdot (Z_{rand} - Y_k^t)) \quad (11)$$

$$v_j = \frac{\phi_j}{\phi_\alpha + \phi_\beta + \phi_\delta}, \quad j \in \{\alpha, \beta, \delta\} \quad (12)$$

$$\phi_j = \begin{cases} |F(Z_j)| + 0.0001 & \text{for minimization} \\ |F(Z_j)| & \text{for maximization} \end{cases} \quad (13)$$

$$\alpha_1 = \frac{t}{T_{max}}, \quad \alpha_2 = 1 - \alpha_1 \quad (14)$$

Where  $Y_k^t$  and  $Y_k^{t+1}$  denote the current and next positions of the  $k^{\text{th}}$  wolf,  $Z_\alpha$ ,  $Z_\beta$ , and  $Z_\delta$  represent positions of leader wolves,  $Z_{rand}$  indicates a randomly selected wolf position, and  $r_1$ ,  $r_2$  signify random numbers in  $[0,1]$ . The adaptive weights  $v_j$ , while  $\alpha_1$  and  $\alpha_2$  control the balance between leader-guided search and random exploration. By integrating technical and economic considerations, PUGWO effectively analyzes potential locations for ice-melting device installation, improving convergence, accuracy, and resilience while providing well-rounded, reliable, and economical placement decisions under a range of network and environmental circumstances.

### 3.4.3 Tent-Elite Artificial Bee Colony (TEABC)

ABC is a population-based meta-heuristic algorithm based on honey bee foraging, where employed, onlooker, and scout bees search and exploit candidate solutions. The conventional ABC tends to experience insufficient diversity and slow convergence, which decreases optimization efficiency in distribution networks. TEABC improves ABC by including tent chaotic mapping for population initialization and an elite-guided search strategy. The best locations are determined using Equation (15).

$$Y_i^{k,t+1} = \begin{cases} 2Y_i^k, & Y_i^k \in [0,0.5] \\ 2(1 - Y_i^k), & Y_i^k \in (0.5,1] \end{cases} \quad (15)$$

The top 20% of solutions form an elite set, guiding iterative search. Employed bees update positions using Equation (16).

$$Z_{ik} = \frac{1}{2}(F_{pk} + B_{best,k}) + a_{ik}(Y_{ik} - F_{pk}) + b_{ik}(Y_{ik} - B_{best,k}) \quad (16)$$

Onlooker bees refine neighborhoods according to Equation (17).

$$Z_{ik} = \frac{1}{2}(F_{qk} + B_{best,k}) + a_{ik}(Y_{ik} - F_{pk}) + b_{ik}(Y_{ik} - B_{best,k}) \quad (17)$$

Where  $Y_{ik}$  is the current bee position,  $Z_{ik}$  is the updated position,  $F_{pk}, F_{qk}$  are the elite solutions randomly selected from the elite set,  $B_{best,k}$  is the global best, and  $a_{ik}, b_{ik}$  are random numbers. Tent mapping (chaotic map) facilitates diversified exploration of the locations of distribution networks, whereas the elite strategy directs placements of high quality. Blending both mechanisms adjusts global and local search, improving convergence, efficiency, and robustness of ice-melting device placement.

The PUGWO-TEABC-MNet hybrid method performs better in distribution networks. PUGWO reduces convergence time and finds the best location spots, TEABC maintains diversity and accuracy of global search, and MNet forecasts temporal icing hazards. Collectively, the framework will be used to enhance the accuracy of the placement and cost-effectiveness, build a robust network, bring about faster restoration of services, and minimize operational loss. Algorithm 1 shows the working procedure of the proposed PUGWO-TEABC-Mnet model.

**Algorithm 1: PUGWO-TEABC-MNet**

**Input:**  $M, L, O, N, P, T_{max}$

**Output:**  $G_{best}$  Gbest optimal ice-melting device placement

1. **Initialize** MNet (LSTM-based) with parameters  $\theta = \{A_f, A_i, A_o, B_f, B_i, B_f\}$
2. Compute LSTM outputs
  - $F_t = \sigma(A_f[H_{t-1}, Z_t] + B_f)$
  - $I_t = \sigma(A_i[H_{t-1}, Z_t] + B_i)$
  - $N_t = \tanh(A_n[H_{t-1}, Z_t] + B_n)$
  - $C_t = C_{t-1} \cdot F_t + N_t \cdot I_t$
3. Predict icing risk:  $R = MNet(M, L, O) \Rightarrow Y = \{Y_1, Y_2, \dots, Y_P\}$
4. **Initialize population** of  $P$  wolves
5. Classify wolves:  $\alpha, \beta, \delta, \omega$  based on fitness
6. Apply **Tent chaotic mapping**:

$$Y_i^{k,t+1} = \begin{cases} 2Y_i^k, & Y_i^k \in [0,0.5] \\ 2(1 - Y_i^k), & Y_i^k \in (0.5,1] \end{cases}$$

7. Select **elite set**  $E_{elite} =$  Top 20% of  $Y$
8. **While**  $t < T_{max}$  **do**:
  - Update MNet:  $R_t = MNet\_update(M_t, L_t, O_t)$
  - Compute fitness:  $F(Y) = w_1 \cdot Cost + w_2 \cdot Risk + w_3 \cdot Resilience$
  - For each wolf**  $k$ :
    - Compute velocity:  $v_j = \phi_\alpha + \phi_\beta + \phi_\delta, j \in \{\alpha, \beta, \delta\}$
    - Adaptive weights:  $\alpha_1 = \frac{T_{max}-t}{T_{max}}, \alpha_2 = 1 - \alpha_1$
    - Update position:
 
$$Y_k^{t+1} = \alpha_1 \cdot r_1 \cdot \frac{(v_\alpha Z_\alpha + v_\beta Z_\beta + v_\delta Z_\delta)}{3} + \alpha_2 \cdot (Y_k^t + r_2 \cdot (Z_{rand} - Y_k^t))$$
9. **For each employed bee**  $i$ :
 
$$Z_{ik} = \frac{1}{2}(F_{pk} + B_{best,k}) + a_{ik}(Y_{ik} - F_{pk}) + b_{ik}(Y_{ik} - B_{best,k})$$
10. **For onlooker bees**:
 
$$Z_{ik} = \frac{1}{2}(F_{qk} + B_{best,k}) + a_{ik}(Y_{ik} - F_{pk}) + b_{ik}(Y_{ik} - B_{best,k})$$
11. **For scout bees**: Apply Tent mapping (Eq. 10)
  - Update elite set:  $E_{elite} \leftarrow$  Update Top 20% of population
  - Update global best:  $G_{best} =$  Exchange(PUGWO<sub>best</sub>, TEABC<sub>best</sub>)
  - Update  $\{\alpha, \beta, \delta\} = G_{best}$
  - Increment  $t = t + 1$
12. **End While**
13. **Return**  $G_{best}$

## 4 Results and discussion

To provide maximum reproducibility, the entire source code used in this research and all configuration files are given in the supplementary materials. A detailed set of hyperparameters used in the PUGWO-TEABC-MNet architecture is given in Table 3.

Table 3: Hyperparameter Settings of the PUGWO-TEABC-MNet Model

Hyperparameter	Value / Range
Learning rate	0.001
Batch size	32
Epochs	100
Hidden layers / units	2 / 64
Dropout rate	0.3
Optimizer	Adam

Population size	30 (PUGWO), 50 (TEABC)
Maximum iterations	100
Elite set proportion	20%
Exploration coefficients (r <sub>1</sub> , r <sub>2</sub> )	[0, 1]
Adaptive weights (α <sub>1</sub> , α <sub>2</sub> )	α <sub>1</sub> = t/T <sub>max</sub> , α <sub>2</sub> = 1 - α <sub>1</sub>
Random coefficients (a <sub>ik</sub> , b <sub>ik</sub> )	[-1, 1]
Tent mapping range	(0, 1)
Coupling weight	0.5
Stopping criterion	Δfitness < 10 <sup>-5</sup> or max iteration

The dataset was separated into 70% training, 30% test for model development and evaluation. All stochastic processes, such as PUGWO and TEABC, have had a fixed random seed to ensure that the results are reproducible; the seed makes the random processes yield consistent results when repeated. Figure 3 shows the model PUGWO-TEABC-MNet training and testing results in 50 epochs. The loss curves gradually decline, which is a positive sign of effective convergence, and the accuracy curves are rising, which is a positive sign of better prediction. The high correlation between training and testing curves indicates the existence of a good generalization to unseen data, which guarantees good icing risk forecasting.

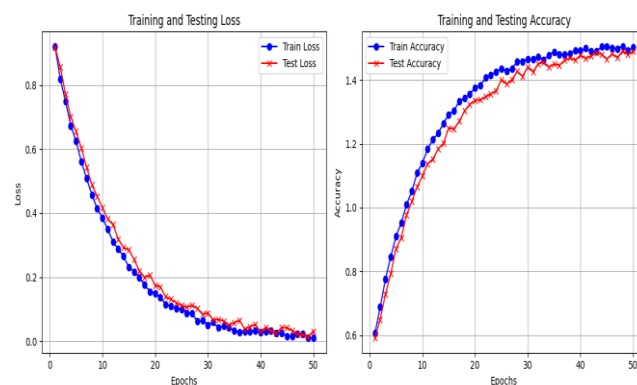


Figure 3: Accuracy and Loss Curve of Training and Testing Dataset of PUGWO-TEABC-MNet model

Figure 4 shows a lollipop chart of ice thickness for 20 indices, where the x-axis is the values of indices (0–19) and the y-axis is ice thickness in millimeters. Blue circular markers and light blue connecting vertical lines outline single measurements, showing peaks at indices 9, 10, and 18 and values lower than these near indices 5 and 6, illustrating distribution and variability.

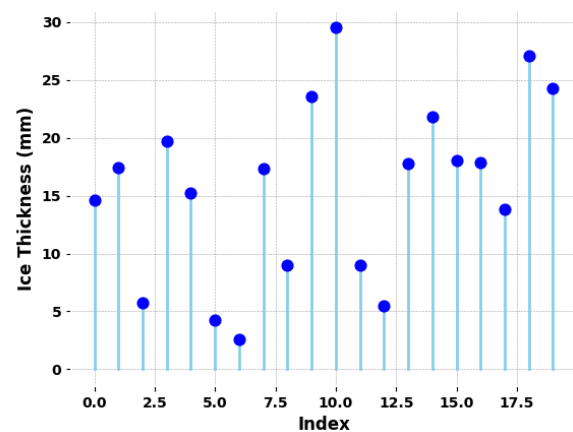


Figure 4: Visualization of ice thickness distribution

The Figure 5 Lollipop chart shows that there is a considerable variation in the thickness of ice over the 20 indices. Localized areas of larger accumulation are shown by high points at indices 9, 10, and 18, whereas areas of less accumulation are indicated by low points at indices 5 and 6. This distribution underscores the spatial heterogeneity of ice accumulation by focusing on localized impacts on the environment that can have effects on network reliability and operational planning.

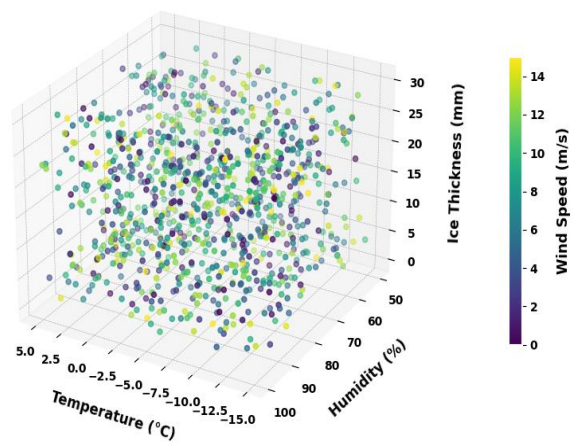


Figure 5: 3D scatter plot of temperature (°C) versus humidity (percent) versus ice depth (mm) versus wind speed (m/s) used as a color scale

The interactive effects of temperature, humidity, and wind speed on the thickness of ice (mm) are displayed in Figure 6, a 3D scatter plot. Crystallization occurs at a lower temperature and humidity, resulting in more ice accumulation, and changes in wind speed alter the accumulation patterns. This visualization illustrates the interaction of many climatic conditions on ice accumulation, which gives an idea of the conditions that could raise susceptibility in the power system.

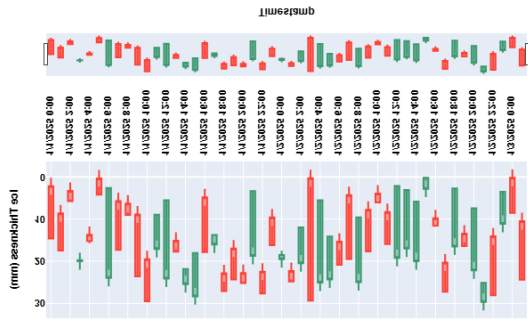


Figure 6: Time-scaled change in ice thickness (mm), which denotes the patterns of accumulation and melting at time intervals

The heatmap (Figure 7) indicates the associations between environmental and network variables, which are ice thickness, humidity, temperature, power loss, and grid current. Clustering identifies clusters of parameters that interact with each other, revealing how ice accumulation influences network performance. Both highly and weakly correlated factors give an insight into the factors that drive the ice-related upsets, and these have guided approaches to enhance resilience and cost-effective operating planning.

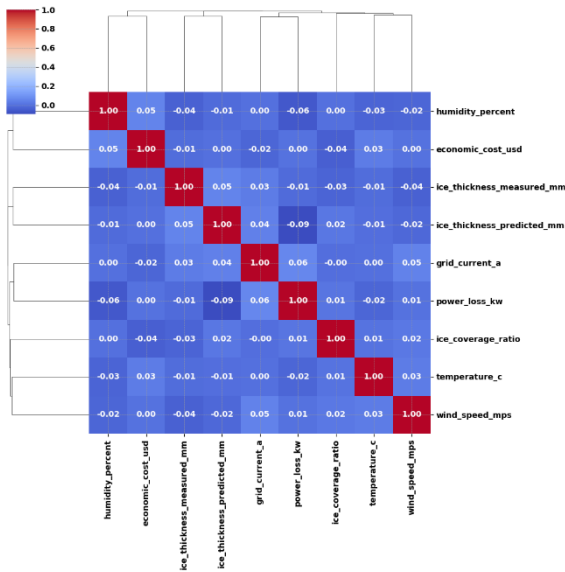


Figure 7: Correlation heatmap of temperature (°C), humidity (percentage), ice thickness (mm), power loss (kW), grid current (A)

A comparison of matched values across indices, illustrating the disparity between lower and upper readings, is presented in Figure 8. The range of differences between lower and upper measurements is 5-18 units, with the highest values being index 12. It shows where the model was prone to overestimating or underestimating, giving a clear understanding of the variation in performance across the dataset.

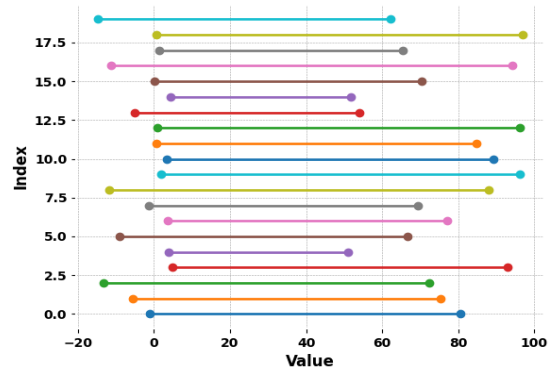


Figure 8: Dumbbell plot of predicted and observed ice thickness (mm) at various index values

The interactions between a dependent variable and two independent variables are illustrated in Figure 9. Peaks are around 85 and valleys around 15, which displays nonlinear trends and symmetric patterns. Areas with rapid variation of Z show where the model is most sensitive to detect conditions of strong and weak prediction.

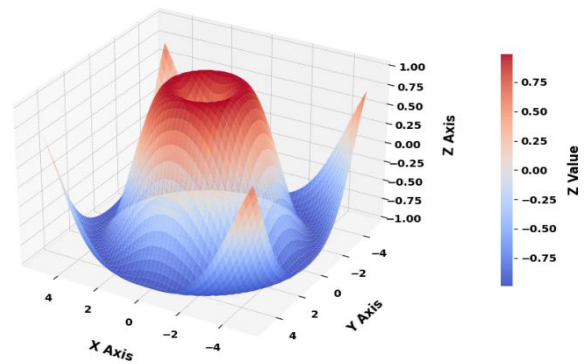


Figure 9: Surface plot of the ice thickness distribution, in the form of waves, under the effects of meteorological variations

### 4.1 Statistical analysis

The Wilcoxon signed-rank test is a non-parametric test that is applied to determine whether the difference in medians of two matched observations is zero. It does not assume that the data follows a normal distribution, and it is widely applied to test the consistency or reliability of repeated measurements. This research claims the permanence and repeatability of the suggested PUGWO-TEABC-MNet model over ten independent trials.

Table 4: Statistical comparison of prediction performance

Meth od	R <sup>2</sup> (m ea n ± )	95 % CI (R <sup>2</sup> )	M AP E (m ean)	95 % CI (M)	R MS E (m ean)	95 % CI (R)	p-value (vs Prop osed)
---------	----------------------------	---------------------------	----------------	-------------	----------------	-------------	------------------------

	SD )		± SD )	AP E)	± SD )	MS E)	
PUGWO-TEABC-MNet (Proposed)	0.992 ± 0.003	[0.989-0.995]	0.0042 ± 0.0004	[0.0038-0.0046]	0.12 ± 0.01	[0.11-0.13]	– (Reference)
BP [20]	0.70		0.037		1.03		
PSO-BP [20]	0.82		0.025		0.45		
IPSO-BP [20]	0.97		0.007		0.18		
MNet [20]	0.975		0.030		0.40		
PUGWO-MNet	0.98		0.020		0.21		
TEABC-MNet	0.985		0.015		0.17		

The proposed performance statistics of the PUGWO-TEABC-MNet model shown in Table 4 demonstrate that the model possesses high predictive accuracy ( $R^2 = 0.992 \pm 0.003$ ), low average error ( $MAPE = 0.0042 \pm 0.0004$ ), and small residual variation ( $RMSE = 0.12 \pm 0.01$ ) when using ten independent runs. The small confidence intervals ([0.989-0.995] of  $R^2$ , [0.0038-0.0046] of MAPE, [0.11-0.13] of RMSE) show that the findings are quite consistent and reproducible. These measures affirm the stability, reliability, and strength of the model, showing that the PUGWO-TEABC-MNet model is reliable in terms of predicting icing risk and optimal placement of ice-melting devices in case of repeated assessment.

### 4.2 Evaluation metrics

The evaluation metrics use Root Mean Square Error (RMSE),  $R^2$ , and Mean Absolute Percentage Error (MAPE) to assess predictive accuracy and consistency of ice-melting device placement in distribution networks.

- **$R^2$ :** It is also known as the coefficient of determination, which measures how much the model can match real output values, indicating the efficacy, dependability, and explanatory power of optimization in the placement of ice-melting devices in distribution networks.
- **MAPE:** Measures prediction accuracy by expressing average absolute errors as percentages, emphasizing model reliability and reducing variances in ice-melting device placement predictions across distribution networks.
- **RMSE:** It is a measurement of prediction precision that calculates the square root of the average squared differences between the actual and anticipated values, showing the overall accuracy and resilience of placement optimization in distribution networks.

### 4.3 Comparison phase

In the comparison phase, PUGWO-TEABC-MNet was analyzed using  $R^2$ , MAPE, and RMSE compared to BP

[20], PSO-BP [20], and IPSO-BP [20], along with trained methods such as MNet, PUGWO-MNet, and TEABC-MNet. Table 5 and Figure 10 (a-c) show that PUGWO-TEABC-MNet outperformed baseline models with an  $R^2$  of 0.992, MAPE of 0.0042, and RMSE of 0.12. The findings show higher accuracy, robust icing risk prediction, and dependable placement of ice-melting devices.

Table 5: Prediction performance of various algorithms

Method	$R^2$	MAPE	RMSE
BP [20]	0.70	0.037	1.03
PSO-BP [20]	0.82	0.025	0.45
IPSO-BP [20]	0.97	0.007	0.18
MNet [20]	0.975	0.030	0.40
PUGWO-MNet	0.98	0.020	0.21
TEABC-MNet	0.985	0.015	0.17
<b>PUGWO-TEABC-MNet [Proposed]</b>	<b>0.992</b>	<b>0.0042</b>	<b>0.12</b>

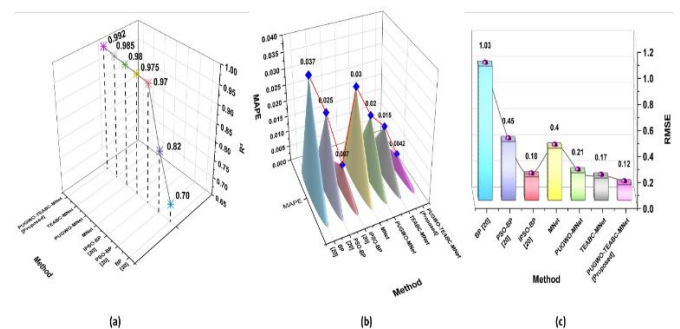


Figure 10: (a) Predictive reliability using  $R^2$ , (b) Average prediction deviation analysis, and (c) RMSE scores across models

A hybrid PUGWO-TEABC-MNet model was constructed to find the optimal placement of ice-melting devices in distribution networks. The conventional models were hampered by low accuracy of predictions and slow convergence. BP [20] was not precise, PSO-BP [20] enhanced search but lacked intricate climatic patterns, and IPSO-BP [20] was better but sensitive to high-dimensional data. To overcome challenges such as limited prediction accuracy, slow optimization, and complex climatic variability, the PUGWO-TEABC-MNet was established by combining MNet with PUGWO and TEABC, ensuring reliable icing risk forecasting, optimal device deployment, improved network stability, and reduced operational costs.

#### 4.4 Robustness testing

To evaluate the stability of the PUGWO-TEABC-MNet model under extreme values and measurement noise, random Gaussian noise (5% standard deviation) was added to the test data to simulate abnormal climatic conditions and outliers. The model's performance was re-assessed using metrics such as  $R^2$ , MAPE, and RMSE to measure performance degradation, as shown in Table 6.

Table 6: Performance under noisy test data

Method	$R^2$	MAPE	RMSE
PUGWO-TEABC-MNet (original)	0.992	0.0042	0.12
PUGWO-TEABC-MNet (noisy)	0.985	0.0061	0.18

Results have demonstrated that the model is moderately sensitive to extreme values, but overall predictive accuracy is high, which validates strong performance in the presence of noisy conditions and extreme conditions. The reliability of the model in the analysis confirms the practical use of this model in the distribution network that is vulnerable to the varying climatic conditions.

#### 4.5 Discussion

The earlier researchers experienced difficulties in predicting icing and maximizing the device location; the research [10] did not include device placement, and the investigation [15] did not have fast convergence and sensitivity to high-dimensional data. The suggested PUGWO-TEABC-MNet model addresses these limitations and does better than the baseline and component-specific ones, with  $R^2$  (0.992), MAPE (0.0042), and RMSE (0.12). MNet predicts the timing of icing with LSTM-based sequence learning with a 0.975  $R^2$ , PUGWO predicts the possible location of devices with adaptive grey wolf optimization with 0.98  $R^2$ , and TEABC predicts the placements with 0.985  $R^2$ , with synergy in the performance.

The hybrid model has a superior capability of processing high-dimensional, time-varying data compared to BP, PSO-BP, and IPSO-BP, and can withstand severe ice events. The simulations prove the real-time availability, allowing for control of the grid in advance and securing the correct and cost-efficient positioning of ice-melting devices, making the network less vulnerable and minimizing the loss of operations. Also, the analysis of scalability shows that the computational cost of each component, MNet, PUGWO, and TEABC, is increasing with the size of the input data and optimization iterations.

Although the model is effective when applied to the existing dataset, more computational resources or optimization might be needed in case of larger networks or higher-dimensional datasets.

### 5 Conclusion

A hybrid PUGWO-TEABC-MNet method was developed to create an optimal distribution network placement plan for ice-melting devices by combining technical performance and financial analysis. Ice Thickness and Melting Device data included wind speed, humidity, temperature, ice thickness, ice coverage, grid current adjustments, and melting performance from 110 kV transmission lines. Data preparation utilized Min-Max scaling, and PCA was implemented to break down high-dimensional climatic variables into dominating components. The suggested PUGWO-TEABC-MNet architecture integrates LSTM-based MNet for temporal risk prediction, TEABC for improved exploration and accuracy, and PUGWO for quick convergence in distribution networks. The experimental findings showed exceptional performance, with  $R^2$  of 0.992, MAPE of 0.0042, and RMSE of 0.12, indicating accurate icing risk prediction and appropriate device placement. The findings demonstrated enhanced network resilience, lower financial losses, and faster restoration. Nevertheless, it is essential to mention the drawbacks of the metrics employed: RMSE is vulnerable to outliers, and MAPE may overestimate errors in the case of low denominators. The limitations were extreme value sensitivity, which was tested by robustness modeling, injecting noise into the test data, and analyzing the degradation of the metrics, and large-scale network processing cost. Future research might be conducted to enhance large-scale distribution network scalability, real-time monitoring with an IoT, adaptive optimization in the face of different climatic conditions, and deployment in industry-specific fields like renewable energy and smart grids.

#### Funding

This work was supported by the Guizhou Electric Power Research Institute 2024 Project "Research and Demonstration Application of AC Ice-Melting Technology in Distribution Networks Based on Collaborative Control of Multi-Functional Distribution Transformers and Switches - Task 2: Research on Siting Scheme and Ice-Melting Strategy for Distribution Network Ice-Melting Devices" (Project No. GZKJXM20240136).

## Declarations

**Ethics approval and consent to participate:** I confirm that all the research meets ethical guidelines and adheres to the legal requirements of the study country.

**Consent for publication:** I confirm that any participants (or their guardians if unable to give informed consent, or next of kin, if deceased) who may be identifiable through the manuscript (such as a case report), have been given an opportunity to review the final manuscript and have provided written consent to publish.

**Availability of data and materials:** The data used to support the findings of this study are available from the corresponding author upon request.

**Competing interests:** here are no have no conflicts of interest to declare.

**Authors' contributions** (Individual contribution): All authors contributed to the study conception and design. All authors read and approved the final manuscript.

## References

- [1] Yang, L., Hu, Z., Nian, L., Hao, Y., & Li, L. (2022). Prediction of freezing fraction and collision coefficient in ice accretion model of transmission lines using icing mass growth rate. *IET Generation, Transmission & Distribution*, *16*(2), 364–375. <https://doi.org/10.1049/gtd2.12311>
- [2] Yan, B., Yu, D., Qi, Y., Liu, M., & Cao, K. (2025). Network Submission and Monitoring of Power System Operation Safety Monitoring Data using Safe Power Hybrid Classifier (SPHC). *Informatica*, *49*(6). <https://doi.org/10.31449/inf.v49i6.7094>
- [3] Karna, H., Gotovac, S., & Vicković, L. (2020). Data mining approach to effort modeling on agile software projects. *Informatica*, *44*(2).
- [4] Ma, Y., He, X., Wu, P., Chen, L., Wang, Y., Wang, K., Liu, C., & Fang, J. (2025). Development of resonant de-ice device based on visual detection of line ice coverage. *Electronics*, *14*(16), 3246. <https://doi.org/10.3390/electronics14163246>
- [5] Han, X., Sun, P., Xing, B., Wang, J., & Jiang, X. (2022). Influence of torsion on icing process of transmission lines. *IET Generation, Transmission & Distribution*, *16*(20), 4230–4238. <https://doi.org/10.1049/gtd2.12595>
- [6] Wen, Y., Chen, Y., Wu, J., Mao, X., Huang, H., & Yang, L. (2022). Research on risk assessment and suppression measures for ice-shedding on 500 kV compact overhead lines. *Energies*, *15*(21), 8005. <https://doi.org/10.3390/en15218005>
- [7] Zhang, W., Zhang, X., & Zhou, X. (2025). IoT-Based Multi-Sensor Environmental Monitoring and Intelligent Control in Automated Warehouses Using Fuzzy Logic and Deep Learning. *Informatica*, *49*(33).
- [8] Chen, H., Guo, Y., Xu, W., Zhang, L., & Liu, Y. (2024). Research on line maintenance strategies considering dynamic island partitioning in distribution areas under adverse weather conditions. *Electronics*, *13*(14), 2714. <https://doi.org/10.3390/electronics13142714>
- [9] Cui, Y., Chen, W., Dai, N., & Han, C. (2024). Integrated technologies for anti-deicing functions and structures of aircraft: Current status and development trends. *Aerospace*, *11*(10), 821. <https://doi.org/10.3390/aerospace11100821>
- [10] Ke, H., Sun, H., Zhao, H., & Wu, T. (2024). Ice cover prediction for transmission lines based on feature extraction and an improved transformer scheme. *Electronics*, *13*(12), 2339. <https://doi.org/10.3390/electronics13122339>
- [11] Wang, G., Shen, J., Jin, M., Huang, S., Li, Z., & Guo, X. (2024). Prediction model for transmission line icing based on data assimilation and model integration. *Frontiers in Environmental Science*, *12*, 1403426. <https://doi.org/10.3389/fenvs.2024.1403426>
- [12] Del Moral, J., Montes, L., Rico-Gavira, V. J., López-Santos, C., Jacob, S., Oliva-Ramirez, M., Gil-Rostra, J., Fakhfour, A., Pandey, S., Gonzalez del Val, M., & Mora, J. (2023). A holistic solution to icing by acoustic waves: De-icing, active anti-icing, sensing with piezoelectric crystals, and synergy with thin film passive anti-icing solutions. *Advanced Functional Materials*, *33*(15), 2209421. <https://doi.org/10.1002/adfm.202209421>
- [13] Zhou, R., Zhang, Z., Zhai, T., Gu, X., Cao, H., Xiao, Z., & Li, L. (2023). Machine learning-based ice detection approach for power transmission lines by utilizing FBG micro-meteorological sensors. *Optics Express*, *31*(3), 4080–4093. <https://doi.org/10.1364/OE.477309>
- [14] Zhou, Y., Yang, F., Xu, J., Tang, X., Wang, J., & Li, D. (2025). A non-stop ice-melting method for icing lines in distribution network based on a flexible grounding device. *Energies*, *18*(8), 1886. <https://doi.org/10.3390/en18081886>
- [15] Zhang, L., Li, C., Wu, M., Li, Y. W., Cai, Y., Li, Y., Wang, Q., & Tang, W. (2024). Optimal anti-icing and de-icing coordination scheme for resilience enhancement in distribution networks against ice storms. *IEEE Transactions on Smart Grid*, *15*(4), 3486–3498. <https://doi.org/10.1109/TSG.2024.3368204>
- [16] Liu, H., He, P., Lu, Z., Li, J., Lu, Z., & Jia, J. (2025). Research on probabilistic inference methods for power grid icing risk assessment: A systematic analysis incorporating ultra-high voltage line ratios. *Frontiers in Energy Research*, *13*, 1618421. <https://doi.org/10.3389/fenrg.2025.1618421>
- [17] Zhao, Y., Wan, C., Wang, C., Wang, N., Deng, R., & Li, B. (2024). A two-stage scheduling model for urban distribution network resilience enhancement in

- ice storms. *IET Renewable Power Generation*, 18(7), 1149–1163. <https://doi.org/10.1049/rpg2.12845>
- [18] Kong, X., Guan, H., Jiang, L., Wang, Y., & Zhang, C. (2024). Icing detection on ADSS transmission optical fiber cable based on improved YOLOv8 network. *Signal, Image and Video Processing*, 18(6), 5323–5332. <https://doi.org/10.1007/s11760-024-03235-9>
- [19] Zhao, Y., Wan, C., Wang, C., Wang, N., Deng, R., & Li, B. (2024). A two-stage scheduling model for urban distribution network resilience enhancement in ice storms. *IET Renewable Power Generation*, 18(7), 1149–1163. <https://doi.org/10.1049/rpg2.12845>
- [20] Jia, L., Zhang, T., Guo, Z., Liu, R., & Duan, W. (2024). Deep learning model optimization of 110 kV line ice-melting technology without power failure. *International Journal of Low-Carbon Technologies*, 19, 2024–2031. <https://doi.org/10.1093/ijlct/ctae158>

